Science of the Total Environment 943 (2024) 173696

Contents lists available at ScienceDirect

Science of the Total Environment

journal homepage: www.elsevier.com/locate/scitotenv

Limited sensitivity of permafrost soils to heavy rainfall across Svalbard ecosystems

R.Í. Magnússon [a,*], S. Schuuring [b,c], A. Hamm [d,e], M.A. Verhoeven [f,g], J. Limpens [a], M.J.E.E. Loonen [h], S.I. Lang [b]

[a] Plant Ecology & Nature Conservation Group, Wageningen University & Research, Droevendaalsesteeg 3a, 6708PB Wageningen, the Netherlands
[b] Department of Arctic Biology, the University Centre in Svalbard, P.O. Box 156, N-9171 Longyearbyen, Svalbard, Norway
[c] Natural History Museum, University of Oslo. P. O. Box 1172, Blindern, 0318 Oslo, Norway
[d] Department of Physical Geography, Stockholm University, SE-106 91 Stockholm, Sweden
[e] Bolin Centre for Climate Research, Stockholm University, SE-106 91 Stockholm, Sweden
[f] Netherlands Institute of Ecology, Droevendaalsesteeg 10, 6708 PB Wageningen, the Netherlands
[g] Department of Coastal Systems, Royal Netherlands Institute for Sea Research, PO Box 59, 1790 AB Den Burg, Texel, the Netherlands
[h] Arctic Centre, University of Groningen, PO Box 716, 9700 AS Groningen, the Netherlands

HIGHLIGHTS

- Increases in heavy rainfall in the Arctic may have diverging effects on permafrost.
- We simulated heavy rain at variable times and locations on Svalbard using irrigation.
- Effects of rainfall on soil thermal regime were small, site-specific and short-lived.
- Role of local environmental conditions overruled effects of irrigation.
- This fits recent evidence that maritime permafrost regions are less sensitive to rain.

GRAPHICAL ABSTRACT

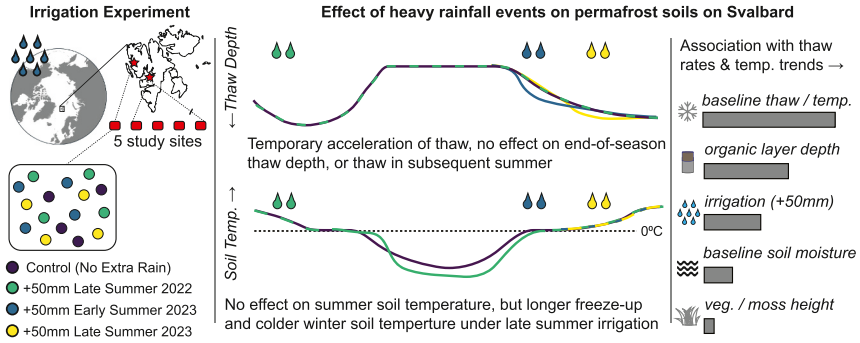

ARTICLE INFO

Editor: Jose Julio Ortega-Calvo

Keywords:
Irrigation
Arctic
Soil thermal regime
Landscape heterogeneity

ABSTRACT

Together with warming air temperatures, Arctic ecosystems are expected to experience increases in heavy rainfall events. Recent studies report accelerated degradation of permafrost under heavy rainfall, which could put significant amounts of soil carbon and infrastructure at risk. However, controlled experimental evidence of rainfall effects on permafrost thaw is scarce. We experimentally tested the impact and legacy effect of heavy rainfall events in early and late summer for five sites varying in topography and soil type on the High Arctic archipelago of Svalbard. We found that effects of heavy rainfall on soil thermal regimes are small and limited to one season. Thaw rates increased under heavy rainfall in a loess terrace site, but not in polygonal tundra soils with higher organic matter content and water tables. End-of-season active layer thickness was not affected. Rainfall application did not affect soil temperature trends, which appeared driven by timing of snowmelt and organic layer thickness, particularly during early summer. Late summer rainfall was associated with slower freeze-up and colder soil temperatures the following winter. This implies that rainfall impacts on Svalbard

* Corresponding author.
E-mail address: runa.magnusson@wur.nl (R.Í. Magnússon).

https://doi.org/10.1016/j.scitotenv.2024.173696
Received 21 March 2024; Received in revised form 15 May 2024; Accepted 31 May 2024
Available online 5 June 2024

permafrost are limited, locally variable and of short duration. Our findings diverge from earlier reports of sustained increases in permafrost thaw following extreme rainfall, but are consistent with observations that maritime permafrost regions such as Svalbard show lower rainfall sensitivity than continental regions. Based on our experiment, no substantial in-situ effects of heavy rainfall are anticipated for thawing of permafrost on Svalbard under future warming. However, further work is needed to quantify permafrost response to local redistribution of active layer flow under natural rainfall extremes. In addition, replication of experiments across variable Arctic regions as well as long-term monitoring of active layers, soil moisture and local climate will be essential to develop a panarctic perspective on rainfall sensitivity of permafrost.

1. Introduction

Permafrost underlies a significant proportion (15 %) of land surface in the Northern hemisphere (Obu, 2021), and is subject to thaw and degradation in response to a changing climate (IPCC, 2021; Smith et al., 2022). Over the past decades, permafrost soils have shown increases in ground temperatures up to depths of tens of meters, and increased maximum depth of seasonal thaw of the topmost permafrost layer ("active layer thickness" or ALT) (Biskaborn et al., 2019; Smith et al., 2022). With permafrost soils storing 1460–1600 Pg of carbon, of which 1035 Pg is stored in the top 3 m (Tarnocai et al., 2009; Hugelius et al., 2014), the risk of climate feedback due to carbon mobilization from previously frozen ground is significant (Miner et al., 2022; Schuur et al., 2022). Permafrost thaw can additionally alter local topography, hydrology and plant communities and destabilize Arctic infrastructure and communities, particularly in case of ice-rich permafrost (Teufel and Sushama, 2019; Heijmans et al., 2022; Hjort et al., 2022). However, the landscape dynamics, hydrology and carbon balance specific to permafrost ecosystems are still poorly represented in global climate models and carbon emission scenarios (IPCC, 2021; Natali et al., 2021; Miner et al., 2022).

Beside increases in air temperature, recent studies suggest that heavy rainfall events may have adverse impacts on the thermal state and stability of permafrost soils (Neumann et al., 2019; Douglas et al., 2020; Christensen et al., 2021; Magnússon et al., 2022; Hamm et al., 2023). Observed impacts include deeper thaw of ice-rich permafrost (Magnússon et al., 2022), increased active layer temperatures in thermokarst bogs (Neumann et al., 2019) and thaw slumping (Kokelj et al., 2015), which generally results in ground disturbance, reduced carbon uptake and enhanced greenhouse gas emissions (Kokelj et al., 2015; Neumann et al., 2019; Christensen et al., 2021). Reanalysis data indicate a 24 % increase in rainfall in the Arctic over the past 40 years (AMAP, 2021). Climate projections suggest further increases in Arctic rainfall due to combined effects of increased precipitation and warming (Bintanja and Andry, 2017), as well as increased year-to-year variability and extremes in summer rainfall (Kusunoki et al., 2015; Bintanja et al., 2020). Model studies show that rainfall increases could contribute substantially to future loss of permafrost extent and active layer deepening (Karjalainen et al., 2019; Mekonnen et al., 2021). In particular, neglecting the direct heat transfer from rainwater into permafrost soils could result in underestimation of future increases in active layer thickness due to vertical and lateral transport of heat in permafrost soils (Mekonnen et al., 2021). Lateral subsurface flow can additionally drive spatially diverging responses across topographical gradients (Neumann et al., 2019; Hamm and Frampton, 2021; Eklof et al., 2024). However, the limited availability of empirical evidence of the effects of rainfall infiltration on permafrost thaw currently prevents realistic simulation of future permafrost extent under changing precipitation patterns (Smith et al., 2022).

The limited body of available field-based studies shows diverging effects of heavy rainfall events on soil temperatures and active layer thickness in permafrost ecosystems. Current evidence suggests that permafrost in continental regions is more prone to accelerated thaw under heavy rainfall, while little effects are observed in maritime regions (Hamm et al., 2023, and references therein). This has been attributed to larger increases in thermal conduction upon wetting under warmer and drier summer conditions in continental permafrost sites compared to maritime sites (Hamm et al., 2023). Beside regional contrasts, small-scale local heterogeneity in topography, hydrology and vegetation can induce substantial within-site variability in permafrost response to climatic factors (Jorgenson et al., 2010; Blok et al., 2011; Hamm and Frampton, 2021; Heijmans et al., 2022; Smith et al., 2022; Von Oppen et al., 2022). Higher shrub and bryophyte cover have been associated with reduced seasonal thaw and stronger decoupling of air and ground temperatures, mainly as a result of summer shading and build-up of organic layers with relatively low heat conductivity (Gornall et al., 2007; Heijmans et al., 2022, Von Oppen et al., 2022). Canopies of shrubs or other taller vegetation may additionally intercept rainfall (Zwieback et al., 2019), thereby reducing heat advection into soils by reducing infiltration of (relatively warm) rainfall (Mekonnen et al., 2021; Hamm et al., 2023). These findings highlight that regional climate contrasts as well as local ecosystem properties likely regulate the rainfall-sensitivity of permafrost and that regionally and locally distributed field data are necessary to inform projections of permafrost stability under climate change. However, many studies to date have relied on few or single monitoring sites to derive the impact of naturally occurring heavy rainfall events on permafrost ground temperatures (Iijima et al., 2010; Neumann et al., 2019; Zhang et al., 2021). Few studies have deliberately included spatial replication over landscape gradients to quantify local variability in rainfall sensitivity of permafrost (Douglas et al., 2020), or considered the role of seasonal timing of rainfall.

Here, we experimentally tested whether heavy rainfall events in summer affect permafrost thaw and soil temperatures in five sites across Svalbard, representing a variety of ecosystems with variable hydrological position and soil type. This High Arctic archipelago has shown increases in rainfall and heavy rainfall events in past decades (Hanssen-Bauer et al., 2019; AMAP, 2021). Svalbard and other High Arctic sites are underrepresented within the current evidence base of heavy rainfall impacts on soil thermal regimes, which is largely based on studies in continental Alaska and Siberia, Greenland and the Tibetan Plateau (Lopez et al., 2010; Neumann et al., 2019; Douglas et al., 2020; Luo et al., 2020; Magnússon et al., 2022; Hamm et al., 2023). Over recent decades, permafrost thaw depths on Svalbard have increased by 0.7 cm per year (Adventdalen, Strand et al., 2021), and borehole temperatures have shown increases of 0.09–0.07 °C per year (Adventdalen, 10-20 m depth) (Isaksen et al., 2022) to 0.18 ± 0.07 °C per year (Ny-Ålesund, 138 cm depth) (Boike et al., 2018). It is currently unknown how anticipated further increases in rainfall (Hanssen-Bauer et al., 2019) may affect permafrost thaw and soil temperatures. We simulated a doubling of average summer rainfall (50 mm, June–August) using a controlled irrigation set-up with variable timing of irrigation within the season. We expected that the effects of anticipated rainfall increases in a highly maritime environment such as Svalbard could be less pronounced (Hamm et al., 2023) compared to earlier studies in predominantly continental regions reporting accelerated permafrost thaw and subsoil warming (Lopez et al., 2010; Douglas et al., 2020; Magnússon et al., 2022). We further expected that effect size may vary with seasonal timing of rainfall events, and that legacy effects may be observed in the following summer season (Magnússon et al., 2022). We incorporated in situ environmental measurements, to evaluate whether rainfall impacts differ across landscape gradients (e.g. topography, soil characteristics and vegetation traits). We thereby aimed to contribute to improved

panarctic forecasting of permafrost degradation under increased Arctic rainfall extremes (Hamm et al., 2023) and to provide novel insights into local drivers of permafrost rainfall sensitivity.

2. Materials & methods

2.1. Study system

We conducted our controlled irrigation experiments in two valleys (Adventdalen and Endalen) close to Longyearbyen (78.22°N, 15.63°E), and in Ny-Ålesund (78.92°N, 11.92°E) on the High Arctic archipelago of Svalbard (Fig. 1a). The study areas have a relatively mild, maritime climate compared to other regions at similar latitude, with mean annual temperatures of −3.64 °C and −3.98 °C and total annual precipitation of 198 mm and 471 mm for Longyearbyen Airport (Norwegian Meteorological Institute, station SN99840) and Ny-Ålesund (station SN99910), respectively, over the past three decades (1993–2022). Mean summer (June–August) temperatures and precipitation are 5.67 °C and 4.49 °C, and 50 mm and 83 mm, respectively, for the same decades. Permafrost on Svalbard is generally 100 m (coastal zones) to 500 m (mountainous zones) thick, and its thermal dynamics are strongly driven by topography and insulation by the snowpack in winter (Humlum et al., 2003).

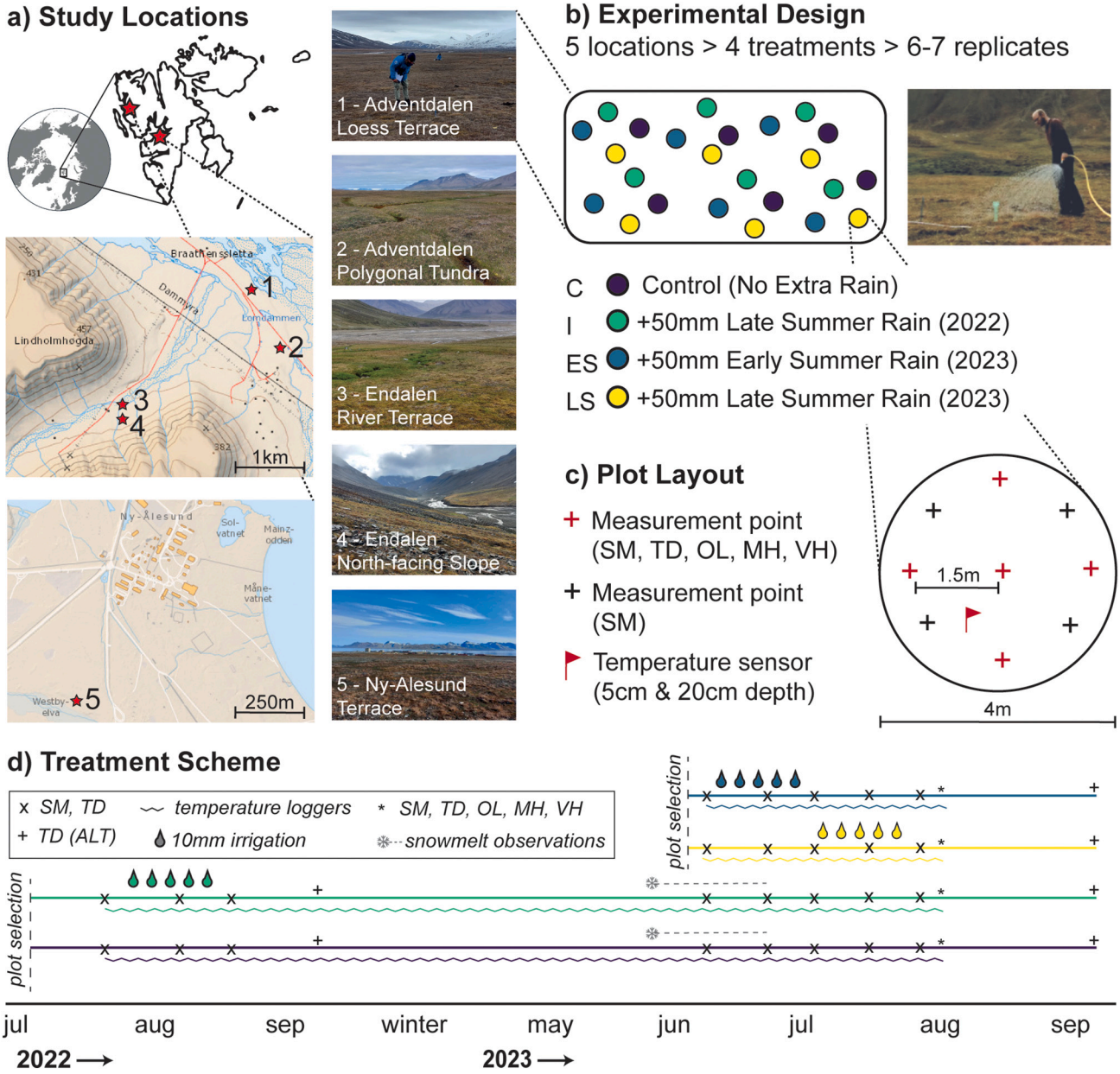

Fig. 1. Experimental Design. a) Study locations were set out close to Longyearbyen (two sites in Adventdalen, two in Endalen) and Ny-Ålesund. Topographical maps from www.toposvalbard.npolar.no. b) At each location, six or seven replicates for each treatment were set out, with one control treatment and three irrigation treatments with rainfall simulation at different moments. Plots were placed at least 5 m apart. c) Irrigation was supplied in 4 m diameter circular plots. In each plot, soil moisture (SM) was measured regularly in nine points at 1.5 m distance from the plot center. Thaw depth (TD) was measured regularly at five points in each plot. In 2023, we measured organic layer depth (OL), moss height (MH) and vegetation height (VH) once at the same points as thaw depth. In each study location, three replicates of each treatment were supplied with a temperature sensor at 5 cm and 20 cm depth. Sensors were placed at approximately 1.5 m from the plot center at variable (representative) locations within the plot. d) Timeline of the experiment and measurements (but see exceptions under 2.2.2). Control and Irrigation plots were set out in 2022 and monitored throughout 2022–2023, while early summer and late summer irrigation plots were added in 2023. Symbols and abbreviations (as in c) indicate timing of different measurements.

Seasonal thaw of permafrost on Svalbard is relatively deep compared to other Arctic regions, with a reported average active layer thickness (ALT) of 99 cm (Strand et al., 2021).

2.2. Experimental design

For our irrigation study, five experimental locations (Fig. 1a) were chosen in such a way that they reflect contrasts in potential drivers of ALT across Svalbard (e.g. topographic position, soil type, plant community) and were accessible from settlements and roads and situated close to water bodies (streams and ponds) to serve as a water source. These water bodies were assumed to be fed by snowmelt and potentially active-layer ice. Site descriptions are available in Table 1. At each location, 4 m diameter circular plots were set out, which were randomly subdivided into control sites and three treatment levels with different timing of irrigation. We set out six or seven replicates per treatment per location (Fig. 1b, c). To avoid spillover effects, plots were at least 5 m apart and in slope locations (Endalen) we avoided setting out control plots directly downslope from irrigation plots as much as possible (although exact subsurface flow paths were unknown). Plot locations were chosen for visual comparability (vegetation and microtopography) within replicate sets of treatments, but were generally not similar or proximate enough to be considered actual treatment blocks. At the start of the experiment in July 2022, Control (C) and Irrigation (I) sites were set out, and I sites received irrigation between July 22nd and August 6th (Fig. 1d). Permafrost thaw progression was monitored for the remainder of the summer and the summer after to capture potential lagged effects.

To determine whether thaw response differs among rainfall extremes earlier and later in summer, we added plots for two additional treatment levels in early June 2023 in four out of five locations. Half of these received additional rainfall between June 15th and 27th (Early Summer, ES), and the other half received additional rainfall between July 1st and July 13th (Late Summer, LS). Due to later snowmelt in Ny-Ålesund, the ES and LS treatment levels in 2023 at Location 5 were delayed to July 5th - 16th and July 20th - July 30th, respectively. In Location 3, no additional treatments (ES, LS) were added.

We simulated an approximate doubling of average summer rainfall (+50 mm, June–August) using a similar approach as Magnússon et al. (2022). The total amount of irrigation was supplied in cumulative amounts of 10 mm approximately every three days. Based on frequency-intensity distributions generated from precipitation records for Svalbard airport for June–August 1975–2023 (Norwegian Meteorological Institute, station SN99840), summers with 100 mm rainfall or more occur approximately every 30 years, and days with 10 mm rainfall or more occur approximately every other year. Water was supplied from local surface water sources (Table 1, Table S1) using a motor pump and hose with sprinkler head (Fig. 1b), or watering cans. The actual amount of irrigation per session was determined using two rain gauges in the plot or based on the volume of the watering cans. Irrigation water was compared to locally sampled rainwater for main nutrients and found to generally resemble the chemical composition of rainwater. Temperature of the water was measured regularly with a handheld thermometer (summer 2022 and early summer 2023) or submerged iButton temperature loggers (summer 2023) (Table S1).

2.3. Site Instrumentation & Measurements

We measured permafrost thaw depth using manual probing with a metal rod with blunt tip until resistance was felt in five points per plot, using the same five points for each consecutive measurement. This was done to minimize soil disturbance, and comparison of values observed using the same hole or a new hole right adjacent to the old one showed no difference in observed thaw dynamics (*Magnússon, Hamm, Lang, pers. obs.*). The accuracy of mechanical probing is estimated at approximately 1 cm (Streletskiy et al., 2022). Thaw depth records were only completed for Locations 1 and 2 in Adventdalen, which are both flat lowland areas. Rocky soils prevented reliable probing in Locations 3, 4 and 5 in Endalen and Ny-Ålesund. Volumetric moisture content of the top 5 cm of soil was measured in nine points per plot to account for heterogeneity (Fig. 1c). We used a handheld Thetaprobe ML2x moisture sensor (Accuracy 1 %, used in Location 1–4, Adventdalen & Endalen) or W.E.T. type 2 sensor (Accuracy 5 %, used in Location 5, Ny-Ålesund), both coupled to a HH2 moisture meter (all Delta-T Devices, Burwell, UK). The HH2 moisture meters were set to factory-calibrated mineral or organic soil preset, depending on the location. Initial soil moisture and thaw depth measurements were carried out prior to onset of the treatments in 2022 (July 21st - 23rd) for the C and I plots, and prior to the new irrigation treatments in 2023 (June 8th - 12th for ES and July 1st - 2nd at Locations 1–4, June 28th for ES and July 19th for LS at Location 5) in all plots. In plots that were already set out in 2022 (C & I plots), we monitored snowmelt progression over the early summer season in 2023 by repeatedly visiting the plots and noting the percentage snow cover per plot every +/− 3 days. In a subset of three plots per treatment per location, we installed iButton DS1921G-F5# temperature loggers in silicone capsules at 5 cm

Table 1
Description of study sites.

Site	Coordinate	Landform	Topography	Soil Type	Vegetation Description	Irrigation Source
1 - Adventdalen - Loess Terrace	78.1988°N, 15.8438°E	Loess terrace (Strand et al., 2021)	Predominantly flat terrain	Mineral, 2.5 m deposit of silt to fine-grained sand (Strand et al., 2021)	Sparse cover of *Salix polaris*, haircap moss, grasses and forbs. Locally cryptogamic crusts.	Meltwater pond
2 - Adventdalen - Polygonal Tundra	78.1915°N, 15.8615°E	High center polygons	Predominantly flat terrain, microtopographical gradients of polygon troughs and centers	> 30 cm of predominantly organic soil, with gradual transition to finer mineral sediment	Denser cover of grasses, sedges, *Salix polaris* and forbs	Meltwater pond
3 - Endalen - River terrace	78.1847°N, 15.7666°E	River terrace	Predominantly flat, gentle gradient from valley slope (snowbed) to bank of river bed (snow free earlier)	Gravelly to fine mineral sediment overlain by organic layer and moss layer of variable thickness	Moss carpets (predominantly *Sanionia uncinata*), *Salix polaris*, grasses and forbs	Meltwater stream
4 - Endalen - Slope	78.1838°N, 15.7658°E	North-facing Slope	Slope angle of ±9° or 15 %	Gravelly to fine mineral sediment overlain by organic layer and moss layer of variable thickness	Moss carpets of variable thickness and species composition, *Salix polaris*, grasses and forbs. Locally cryptogamic crusts, *Cassiope tetragona* and *Dryas octopetala.*	Meltwater stream (same as 3)
5 - Ny-Ålesund - Terrace	78.9197°N, 11.9174°E	Terrace	Predominantly flat, gentle gradient towards Westbyelva	Weathered bedrock (Miccadei et al., 2016) overlain by shallow layer of coal dust (former mine area) and organic layer	Cryptogamic crusts, sparse cover of *Salix polaris*, grasses, forbs, mosses. Locally dense *Racomitrium* cover.	Meltwater stream (Westbyelva)

and 20 cm depth prior to start of the treatments. These recorded soil temperature every 4 h and 15 min at 0.5 °C resolution (Accuracy 1 %, Maxim Integrated Products, Sunnyvale, California, USA). Due to logistic constraints, Location 5 was only instrumented with temperature loggers prior to the 2023 irrigation treatments. Thaw depth and soil moisture measurements were repeated after 30 mm and 50 mm total irrigation for all treatments in all plots, including treatment plots in which irrigation had already been completed before, in order to account for potential longer-term effects (Fig. 1d). Measurements were carried out at a standardized timing of three days since the last irrigation round. We additionally measured the depths in September, as an indication of maximum end-of-season thaw depth or ALT. In late July 2023, we recorded organic layer depth and moss layer thickness using a peat corer and ruler, adjacent to the temperature sensors and thaw depth measurement points. In addition, we recorded vegetation height above the measurement points and iButtons using a 12.6 cm diameter plastic pasture disk and ruler. We used these measurements to account for the potential role of local biotic controls on thaw progression and soil thermal dynamics, and to assess whether particular site conditions were associated with higher rainfall sensitivity of permafrost thaw and soil temperature. Fig. 1c-d shows a spatial and temporal schematic overview of measurements and instrumentation per plot. Site descriptions for the experimental locations are available in Table 1, and Figs. S3 – S6 provide detailed overviews of on-site microclimatic conditions, snowmelt and moisture dynamics and characteristics of soils and vegetation.

2.4. Estimated changes to heat fluxes

To account for potential mismatches in thermal inputs due to differences among irrigation water temperatures and average air temperatures (Table S1), we provide an overview of the expected difference in heat advection due to the use of surface water (Table S2). To provide insight into the relative importance of various physical heat transport processes, we compare estimated changes in thermal heat fluxes associated with infiltration of irrigation water (heat advection), changes in topsoil heat conduction under wetting (Table S3, based on soil thermal parameters, observed soil temperature gradients and field-measured moisture content) and latent heat loss due to evaporation (Table S5, using evaporation rates measured in the field with a simplified lysimeter set up similar to Blok et al., 2011). We compare the magnitude of these heat fluxes across the early summer and late summer treatments across treatment locations for further, process-based insight into effects of heavy rainfall on the soil thermal regime. Text S1 describes the methods and sources used to derive these ancillary data.

2.5. Data analysis

We first visualized seasonal progression of thaw depths per location per treatment, as well as daily soil temperature per treatment per location and depth against air temperatures and precipitation (Svalbard Airport & Ny-Ålesund, see *Study System*) for 2022 and 2023. We then used a mixed effects modeling approach to statistically test for differences in various soil temperature derivatives and thaw progression among treatments. This way, we account for repeated measures in a nested spatial set-up (multiple measurement points per plot, nested in locations). We used three-way interaction models with locations, observational periods and treatment as explanatory variables, to avoid multiple testing per location or measurement round. By adding random intercepts per location and testing for treatment-location interactions, we aimed to account for differences in baseline environmental conditions as well as potential differences in rainfall sensitivity among locations. Finally, we use variance partitioning methods to assess the relative contribution of the rainfall treatments, various environmental controls and their interactions on thaw progression and ground temperatures. This way, we aimed to control for variance induced by specific environmental covariates prior to partitioning variance to the treatments, as well as exploring potential interactions between specific environmental covariates and treatments.

2.5.1. Soil temperature trends & derivatives

For the plots instrumented with temperature sensors, we tested whether the treatment affected several soil thermal processes. Temperature trends were calculated to test if soil temperatures developed differently under different wetting scenarios, relative to their baseline temperatures. Cumulative thawing and freezing degree days were used to assess if treatments affected seasonally integrated soil temperatures. Lastly, the duration of the zero-curtain was derived to assess if the treatments affected the latent heat and time required for phase changes during seasonal freeze-thaw processes (Outcalt et al., 1990). These three derivatives were calculated for each plot instrumented with iButtons, for 5 cm as well as 20 cm depth. Text S2 describes how temperature trends, degree day products and zero-curtain duration were derived.

2.5.2. Thaw Depths & Thaw Rates

We compared thaw depths across the different treatments to assess whether heavy rainfall could result in deeper or shallower active layer thaw compared to control sites. This analysis was limited to the locations in Adventdalen (1 & 2) for which probing data could be obtained. In order to assess whether the irrigation treatments might temporarily accelerate or delay thaw progression relative to baseline thaw depth (prior to treatment), we calculated instantaneous thaw rates (cm/day) over the course of the different treatments. We calculated thaw rates as the difference in the depth per point, divided by the number of days in between the measurements. Thaw rates were generated for all treatment periods (late summer 2022, early summer 2023 and late summer 2023), after 30 mm as well as 50 mm irrigation, to account for potential variability in response due to seasonal timing or potentially nonlinear responses to recurring heavy rainfall events. The corresponding time periods are described in Table S8.

2.5.3. Statistical tests of treatment effect

We used linear mixed effects models (LMMs) to evaluate the effect of the different treatments on soil temperature trends, degree day products, zero-curtain duration, thaw depths and thaw rates. Different treatments were initiated in different years, resulting in different availability and observational periods among treatments (see Fig. 1d). Hence, the analysis was split into two sets of LMMs: First, we evaluated differences in the five response variables (temperature trends, degree days, zero-curtain duration, thaw depth and thaw rate) among C & I plots, in summer 2022, winter 2022–2023 and early summer 2023. These models elucidate the same-year effects of late summer irrigation 2022 and potential carry-over effects to following seasons as observed in earlier work (Iijima et al., 2010; Magnússon et al., 2022). Since ES and LS plots were only established in 2023, no data for 2022 is available. These plots were used, together with the control sites, to evaluate whether the same-year effects of treatment on the five response variables might differ depending on timing of treatment (early or late summer). Since most response variables represent repeated measurements in the same plots, and we expected that treatment effects could differ among study locations and soil depths, we built three way interaction models with treatment, location (for thaw depths and thaw rates), soil depth (for soil temperature derivatives) and observational period as fixed terms, and random intercepts to account for nesting of observations in plots and/or locations. The resulting models are specified further in Table S9.

We assessed significance of fixed effects using F-tests on nested models with Kenward-Rogers approximation of degrees of freedom (Halekoh and Højsgaard, 2014). Backwards elimination based on F-tests was used to derive the most parsimonious model, and we visually checked residuals for approximate normality, homogeneity of variance and absence of patterns against fixed and random terms using residual diagnostic plots. If a significant treatment effect was found, or if treatment was involved in a significant interaction term, we performed post-

hoc tests using pairwise comparison against the control treatment, separating comparisons over different locations and measurement moments in case significant interactions were found. We used a multivariate t-distribution correction for multiple testing during pairwise post-hoc tests (Lenth, 2024). The significance criterion was set to $p < 0.05$. We allowed for post-hoc testing for treatment effects with $p < 0.1$. We report p values <0.1 as tendencies. *2.5.4 Variance explained by treatment relative to (a) biotic landscape controls.*

We used variance partitioning to assess the proportion of variance in thaw rates, temperature trends and active layer thickness explained by the treatments, local a (biotic) conditions and interactions between the two. We limited this analysis to data from 2023, to account for the fact that some environmental covariates were only measured in 2023 (see *2.3*). Snowmelt timing was only monitored for C & I plots, so in order to account for timing of thaw onset we used pre-treatment thaw depth (baseline measurement) or pre-treatment mean temperature (averaged over a 24 h period) prior to irrigation application in the corresponding observation period as covariates. We separately compared temperature dynamics to snowmelt timing for C & I plots (Fig. S14). Other covariates we used were soil moisture prior to irrigation application, vegetation height, moss height and organic layer depth. All these (a) biotic conditions were measured at the same five measurement points per plot as thaw depths, or right above the iButton temperature loggers (*see 2.3*). For soil moisture, no measurement was available at the iButton location, so that of the nearest measurement point was taken, with a maximum distance of approximately half a meter. For variance partitioning of active layer thickness, we used seasonally averaged soil moisture rather than pre-treatment soil moisture, to account for fluctuations throughout the season.

For thaw rates per measurement point, we established individual linear mixed effects models per time period (early and late summer treatment 2023, see Table S8) and Location (1 or 2), with a random intercept for individual plots. We then partitioned variance explained by the environmental covariate, treatment and their interaction by fitting random-intercept models for each unique environmental covariate with an incremental fixed structure. We first fitted a model with only the covariate and random effects, then an additive model with the covariate and treatment factor, then a one-way interaction model with covariate and treatment factor. We compared variance explained by fixed effects (marginal R^2) and random effects (conditional R^2, plot or location) (Nakagawa and Schielzeth, 2013) for each resulting model. For temperature trends, we established similar individual linear mixed effects models per time period (early and late summer treatment 2023, Table S8) and depth (5 cm or 20 cm). Temperature trends were not analyzed separately per location to account for the lower number of observations per location (12 observations for each depth, three for each four treatments), and we used location as a random intercept. Since treatment was discontinued in Location 3 (*see 2.2.2*), we only used Locations 1, 2, 4 and 5. For active layer thickness in 2023, only one measurement per plot was available, and we established individual linear models per Location (1 or 2) with an environmental covariate, treatment, and their interaction as fixed terms. Here, we partitioned R^2 to each unique predictor averaged over all possible orders of fitted terms using the 'lmg' metric (Lindeman et al., 1980; Grömping, 2007).

2.5.4. Software

All analyses were performed in Rstudio, using R version 4.2.1. Mixed effects models were implemented using the lmer() function from the lme4 package (Bates et al., 2015). Significance of model terms was determined using Type III ANOVA tables, as implemented in the anova() function in the lmertest package (Kuznetsova et al., 2017). Post-hoc tests and pairwise comparisons were implemented using the emmeans() and contrast() functions from the emmeans R package (Lenth, 2024). Time series decomposition was performed using the auto. Arima() function from the forecast package (Hyndman and Khandakar, 2008). We used the R2part() function from the partR2 package (Stoffel et al., 2021) to partition explained variance over fixed and random model terms in mixed effects models, and the relaimpo package and "lmg" metric (Grömping, 2007) to partition variance among terms in linear models.

3. Results

3.1. Soil thermal regime under simulated heavy rainfall

Daily soil temperatures at 5 cm and 20 cm depth do not show clear patterns of divergence between irrigated and non-irrigated plots in summer 2023 (Fig. 2). Fig. S3 shows full data series from 2022 onwards for C and I plots, including the winter season. Topographically uniform locations (Location 1, 2 and 5, Table 1) show relatively homogeneous soil temperatures, while the slope and river terrace site in Endalen show large heterogeneity in soil temperatures and timing of thaw onset, likely explained by differences in snowmelt timing (Figs. S3, S5). The plots in Ny-Ålesund (Location 5) show relatively high soil temperatures compared to air temperature (Fig. 2).

Soil temperature derivatives show no direct effect of irrigation on soil temperature trends in summer, but do indicate alteration of the soil thermal regime in the following winter season. Soil temperature trends did not differ significantly between control (C) and irrigated (I) plots over the course of the treatment in 2022, nor during early summer of the following year (F-tests, $p > 0.05$, Table S10). We also found no significant differences in soil temperature trends among irrigation treatments with variable timing (C, ES and LS) in 2023 (F-tests, $p > 0.05$, Table S11). We did find differences in degree day products of C and I plots (thawing degree days in late summer 2022, freezing degree days in winter and thawing degree days in early summer 2023). A significant interaction between season and treatment (F-test, $p < 0.05$, Table S12) indicates that this difference varies seasonally, and post-hoc tests indicate significantly more freezing degree days in irrigated plots over winter (I - C = 107 absolute degree-days, MVT-adjusted $p = 0.01$), but no significant contrasts in late summer 2022 or early summer 2023 (MVT-adjusted $p > 0.05$, Table S13, Estimated Marginal Means Fig. S7). Lastly, we found that the treatment in 2022 affected zero-curtain duration, depending on the season. We found a significant interaction between treatment and season (F-test, $p = 0.04$, Table S14), manifesting as a longer zero-curtain duration in autumn and shorter zero-curtain duration in early summer in I plots after irrigation in 2022 (Estimated Marginal Means, Fig. S8). However, post-hoc tests of treatment effect for autumn and spring season separately show no significant contrast in either season (MVT-adjusted $p > 0.05$, Table S15).

3.2. Permafrost thaw progression under experimental heavy rainfall events

Thaw depth data from mechanical probing was available for Locations 1 & 2 in Adventdalen (not for Endalen and Ny-Ålesund due to rocky soils). Visual comparison indicates no strong divergence in thaw depth among treatment and control plots in 2022 or 2023 for these locations (Fig. 3a). Statistical analysis of thaw depths of control (C) and irrigated (I) plots in 2022 (year of treatment) and early 2023 (summer after treatment) revealed no significant contrasts in thaw depth among treatments, nor significant interactions of treatment with Location (1 or 2) or timing of measurement (F-tests, $p > 0.05$, Table S16). Analysis of thaw depths in early summer (ES) and late summer (LS) irrigation plots against control plots (C) in 2023 revealed that treatment effects varied with location and timing of measurement, evident from a significant three-way interaction (F-tests, $p = 0.02$, Table S17). The data show a pattern of deeper thaw in ES plots after early summer treatment, and LS plots after late summer treatment in Location 1 (Estimated Marginal Means, Fig. S9), but pairwise comparison among treatments shows no specific combination of measurement moment and location with significant contrasts ($p > 0.05$ following MVT adjustment, Table S18). The two sites in Adventdalen do show large contrasts in thaw progression

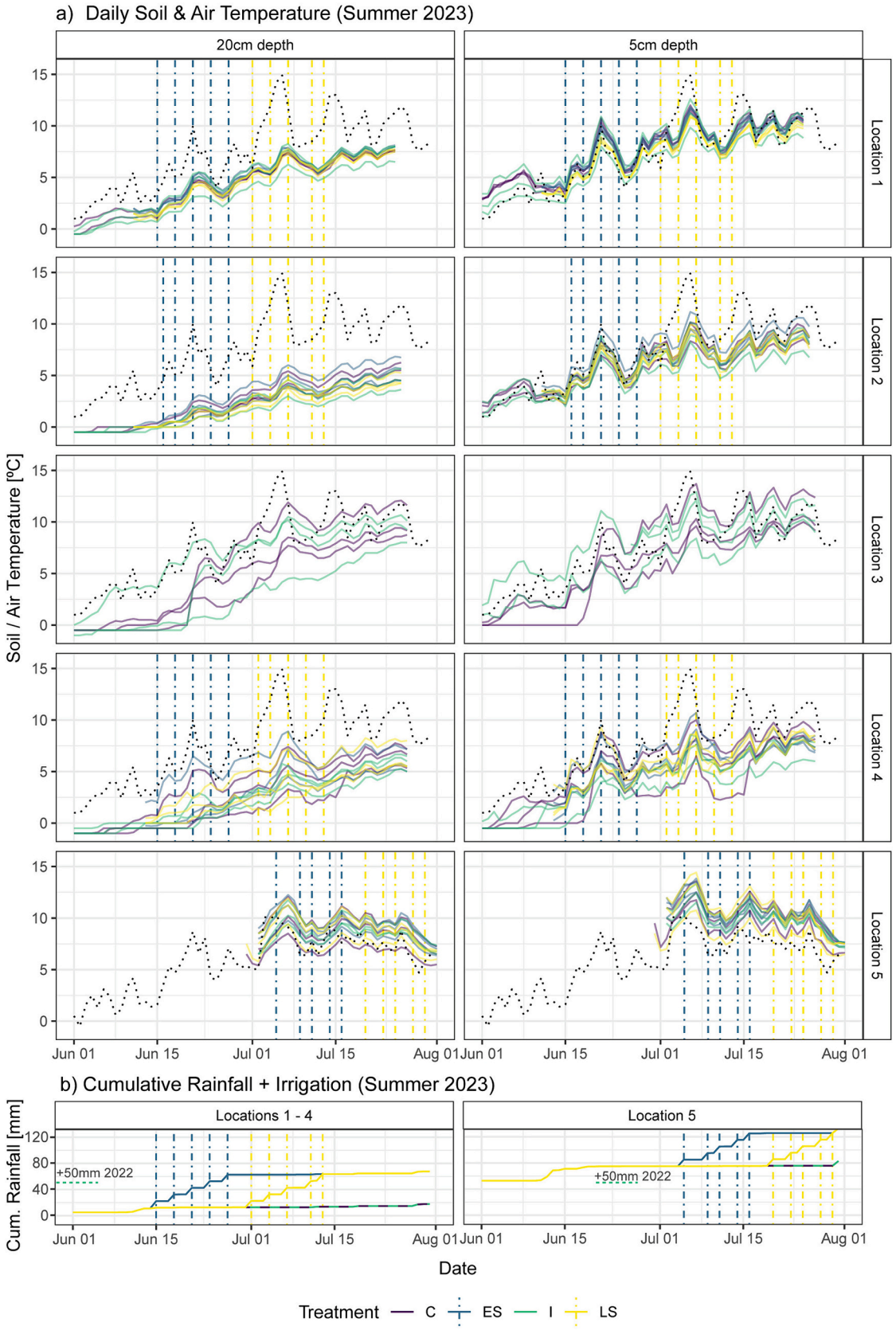

Fig. 2. a) Daily Average Soil Temperature Dynamics over summer 2023 - coloured lines indicate soil temperatures per plot per depth. Black dashed lines indicate air temperature from the nearest weather station (Svalbard Airport for Locations 1–4, Ny-Ålesund for Location 5). Vertical dashed lines indicate the timing of the early summer (ES, blue) and late summer (LS, yellow) treatment per location. Treatments were started later in Ny-Ålesund due to snow presence earlier in the season. Treatment was discontinued in Location 3 in 2023 and only C & I plots were monitored for second-year effects. b) Cumulative rainfall and irrigation for locations in Adventdalen & Endalen (Data from Svalbard Airport, Locations 1–4) and Ny-Ålesund (Location 5).

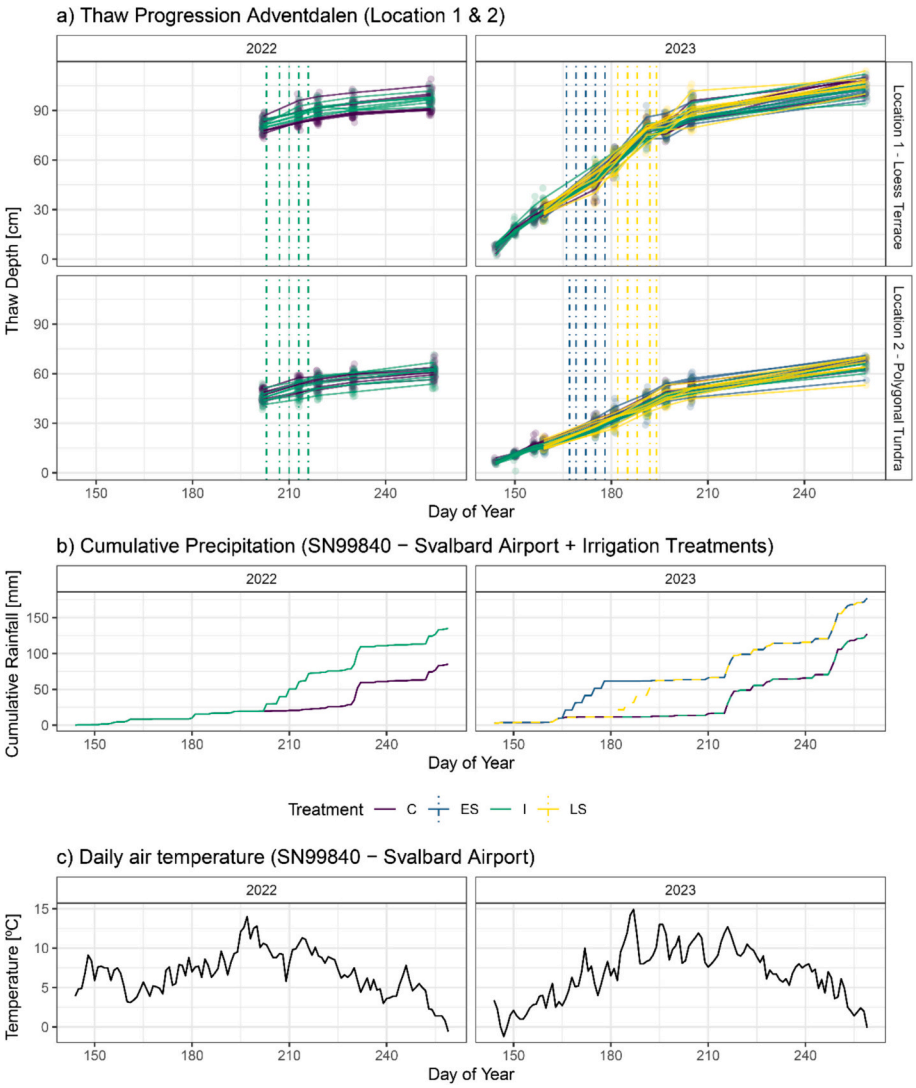

Fig. 3. a) Permafrost seasonal thaw depth in Locations 1 (Loess terrace) and 2 (Polygonal Tundra) in Adventdalen. Lines indicate development of the average thaw depth per plot (n = five measurements per plot), while transparent circles indicate individual measurement points. Vertical dashed bars indicate the timing of supply of each 10 mm rainfall event for each of the three treatments. The "ES" and "LS" lines only appear in 2023, since these locations had not been set out prior to continuation of the experiment in 2023. b) Cumulative ambient rainfall + irrigation treatments over the course of the thaw seasons of 2022 and 2023. c) Average daily air temperature over the course of the thaw seasons of 2022 and 2023.

and end-of-season ALT, with mean ALTs of 96.0 cm and 60.6 cm in 2022 and 104.5 cm and 65.6 cm in 2023 in Locations 1 (Loess Terrace) and 2 (Polygonal Tundra), respectively (averaged over all treatments). Neither of the years showed significant contrasts in ALT among treatments ($p > 0.05$, F-tests, Tables S19 – S20).

Thaw rates indicate a short-lived, local acceleration of thaw during irrigation treatment in 2023 (Fig. 4). Analysis of thaw rates (cm/day) of control (C) and irrigated (I) plots in 2022 (year of treatment) and early 2023 (summer after treatment) revealed no significant contrasts in thaw rates among treatments, nor significant interactions of treatment with Location (1 or 2) or timing of measurement (Table S21, $p > 0.05$, F-tests). Analysis of thaw rates in early summer (ES) and late summer (LS) irrigation plots against control plots (C) in 2023 revealed a significant three-way interaction between treatment, location and moment of measurement (Table S22, $p < 0.05$, F-tests). Consistent with findings for thaw depth (Fig. S9, Table S18), pairwise comparison among treatments per unique combination of measurement moment and location shows a pattern of faster thaw in ES plots in Location 1 during early summer irrigation, and faster thaw in LS plots in Location 1 during late summer irrigation (Fig. 4, S10). Post-hoc tests (following MVT adjustment, Table S23) indicate that plots in Location 1 that received early summer irrigation had thawed 0.27 cm/day faster than control plots, and 0.21 cm/day faster than (still unirrigated) LS plots after 30 mm cumulative early summer irrigation. Treatment contrasts for Location 1 were no longer significant after the full 50 mm early summer irrigation. Plots that received late summer irrigation had thawed 0.20 cm/day faster than control plots over the course of the full 50 mm irrigation application, and 0.19 cm/day faster than ES plots. After 30 mm late summer irrigation, estimated marginal means suggest faster thaw in both ES and LS plots, and LS plots showed a tendency ($p < 0.1$) for faster thaw than C plots in Location 1. Very high overall thaw rates in this period coincide with a temperature spike in early July at the beginning of the LS Treatment (Fig. 3c). No significant contrasts were observed in Location 2 for any of the time periods (Fig. 4).

3.3. Local controls on rainfall sensitivity of permafrost soils

Finally, we compared how local site conditions and treatments jointly contributed to explained variance in thaw rates, temperature trends and active layer thickness over the course of early summer and

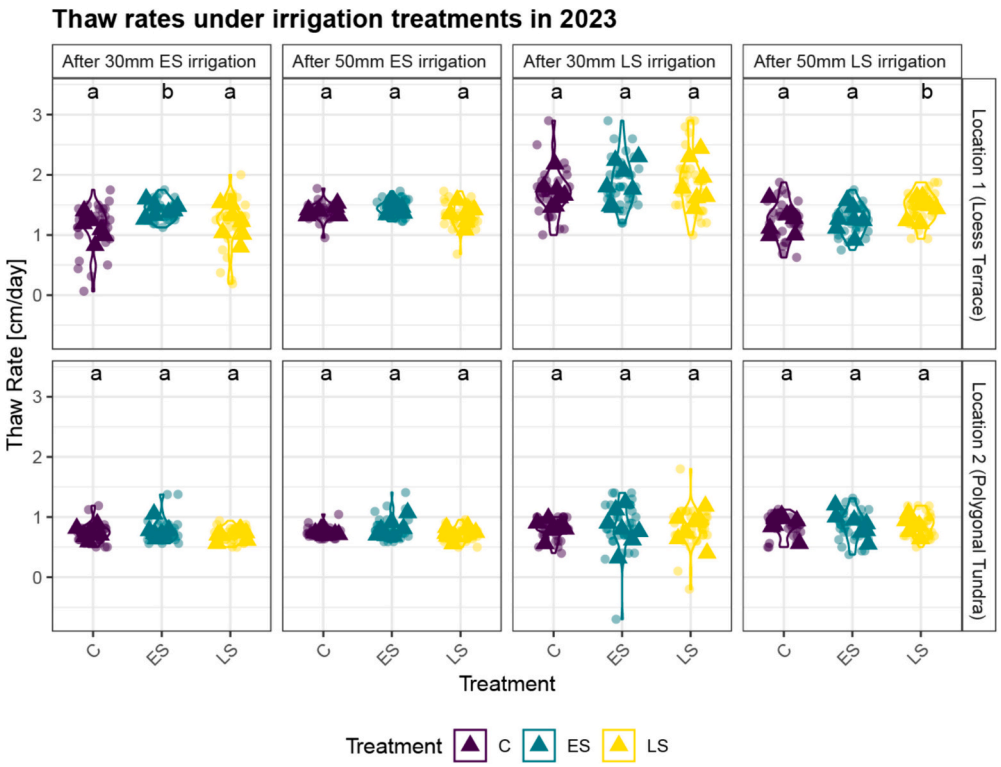

Fig. 4. Violin plots of thaw rates (cm/day) per measurement point relative to baseline measurements. Thaw rates were calculated over the course of the first 30 mm of irrigation and over the course of the full irrigation treatment (50 mm), both for early and for late summer irrigation, in Location 1 (Loess terrace, upper row) and 2 (Polygonal tundra, bottom row) in Adventdalen. Transparent dots indicate individual measurement points (5 per plot), triangles indicate plot averages. Within each panel, violins with a different letter show a significant contrast in thaw rate, based on MVT-adjusted *p*-values and pairwise comparison.

late summer irrigation in 2023 (Fig. 5). Figs. S11 – S13 show supporting scatter plots of soil thermal responses against environmental covariates per plot. In general, only small proportions of variance in thaw rates were attributed to the measured (a) biotic controls and treatment (Fig. 5a). Consistent with Fig. 3, we found that treatment explained more variance in thaw rates in Location 1 (Loess Terrace) than 2 (Polygonal Tundra), although some variance in thaw rates was attributed to treatment in early summer in the polygonal tundra site as well. Apart from treatment, pretreatment thaw depth explained some variability in thaw rates (Fig. 5a), with faster thaw progression in late summer in soils that previously showed shallower thaw (Fig. S11c-d). The limited variance in thaw rates explained by environmental controls may also result from low within-location environmental variability at Locations 1 and 2 (Fig. S11).

For soil temperature trends, the largest proportions of variance were explained by pretreatment temperatures and random intercepts for different locations (Fig. 5b). This likely reflects differences in thaw onset both among the locations, as well as within locations (Fig. S3, S5, S12). Lower pretreatment soil temperatures were associated with higher warming trends (Fig. S12). In all cases, the irrigation treatment explained little variance in temperature trends compared to environmental factors and location-level variance, indicating little influence of rainfall events on in-situ shallow ground temperatures. Particularly in early summer, organic layer thickness explained up to 18 % of variance in temperature trends (Fig. 5b), with thicker organic layers being associated with lower warming trends. In late summer, this influence was only discernible in deeper (20 cm) soil layers. Shallow soil (5 cm) temperature trends in early summer showed some association with treatment, depending on pretreatment moisture levels. Closer inspection shows stronger cooling of previously dry topsoils in early summer in Location 5 (Ny-Alesund) in ES plots, while in other locations ES plots show comparatively high warming trends (Fig. S12a). Here the early summer treatment caused notable wetting of topsoils (Fig. S4), and also coincided with a period of local cooling (Fig. 2).

Finally, we found that active layer thickness (ALT) showed some degree of association with treatment for Location 1 (although no significant differences were evident from statistical tests, Table S20). Specifically, accounting for seasonally averaged soil moisture revealed a relatively stronger increase in ES plots with higher average moisture content over the season, suggesting that a higher degree of effectuated wetting results in stronger treatment response (Fig. S13a). ALT in Location 2 showed no relation to treatment, also after accounting for pre-treatment thaw depth and seasonal moisture content. ALT did show positive association with seasonal moisture content and pre-treatment thaw depth, indicating that wetter sites with deeper early season thaw showed deeper ALT at the end of the summer season, irrespective of irrigation treatment. This may also reflect the higher natural variability in soil moisture observed at Location 2 compared to Location 1 (Figs. S3, S4).

4. Discussion

We found little in-situ effect of heavy rainfall events on permafrost thaw and soil temperatures across a variety of Svalbard ecosystems. None of the experimental treatments significantly affected end-of-season active layer thickness (ALT) in the two experimental sites in Adventdalen. Late season irrigation (late July- early August) in 2022 did not affect permafrost thaw nor soil temperature dynamics, but resulted in longer autumn zero-curtain duration and colder ground temperatures in winter across experimental locations (Adventdalen, Endalen). No lagged effects in subsequent summers were observed. Early (June) and late (July) season irrigation in new plots in Adventdalen in the following year temporarily increased permafrost thaw rates in the loess terrace site, but not in a wetter polygonal tundra area with higher soil organic matter (Fig. 4). The experimental rainfall treatments explained little variance in thaw depth and soil temperature trends compared to

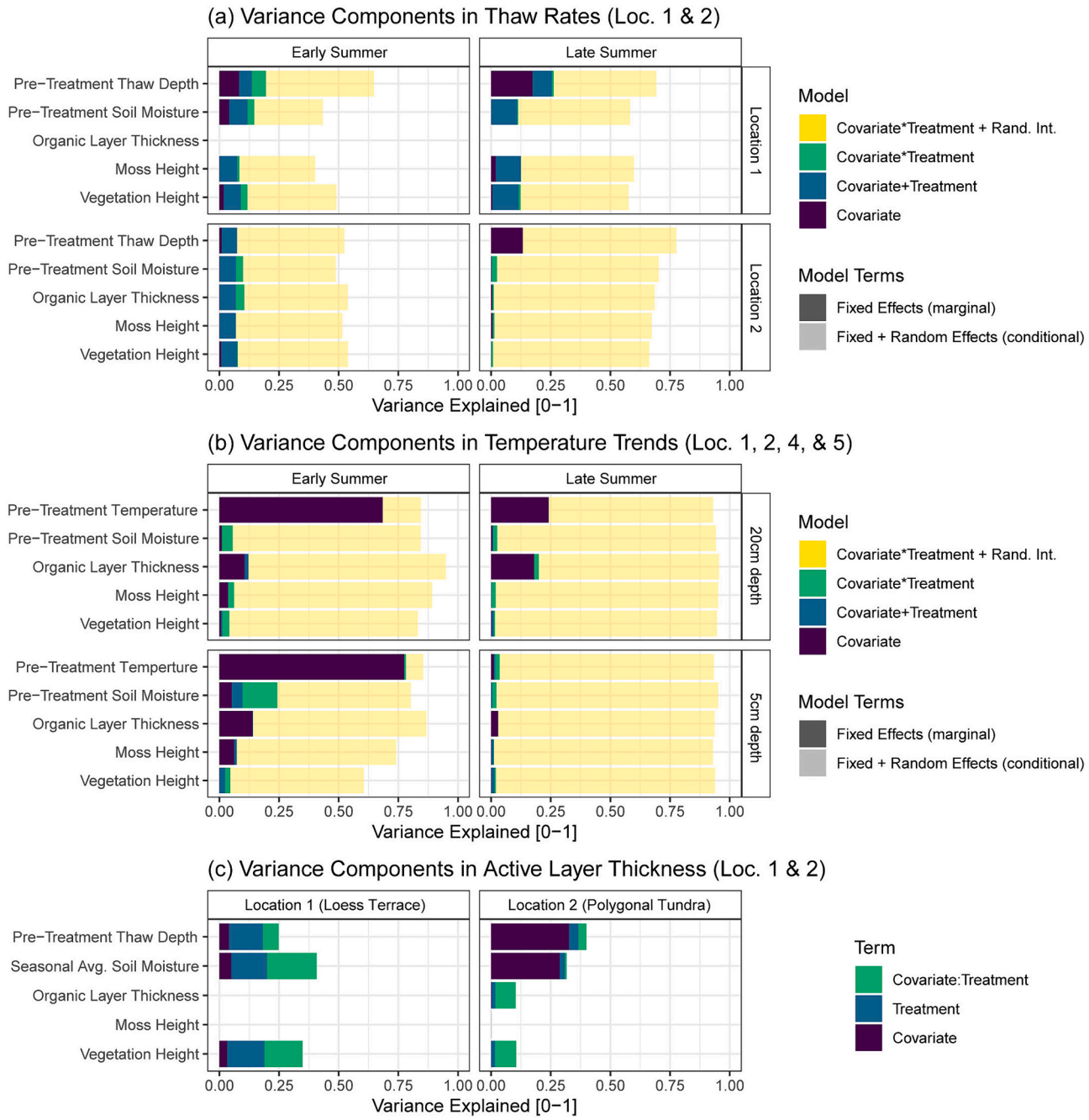

Fig. 5. Variance in permafrost thermal dynamics explained by local site conditions, treatment and their interactions. a) Variance components in thaw rates under early (ES) and late (LS) summer treatment periods in 2023, shown for Location 1 (Loess terrace, Adventdalen) and 2 (Polygonal tundra, Adventdalen). Horizontal bars indicate variance (%) cumulatively explained by the environmental covariate on the y-axes (purple), treatment (blue), their interaction (green) and a random intercept for plot (transparent yellow). b) Variance components in soil temperature trends under early (ES) and late (LS) summer treatment periods in 2023, shown for temperature loggers at 5 cm and 20 cm depth, for all locations combined. Horizontal bars indicate variance (%) cumulatively explained by the environmental covariate on the y-axes (purple), treatment (blue), their interaction (green) and a random intercept for Location (transparent yellow). c) Variance components in Active Layer Thickness (ALT) in Locations 1 and 2. Horizontal bars indicate variance (%) uniquely explained by the environmental covariate on the y-axes (purple), treatment (blue) and their interaction (green). No random intercept was used since only one measurement was taken per plot, see 2.4.5. Variance explained by organic layer thickness and moss height is lacking in places due to general absence of organic layers at Location 1 (a, c), and insufficient variation in moss height in Location 2 (c).

environmental heterogeneity among and within research locations (Fig. 5). While no single (a) biotic variable appeared to fully capture these landscape controls on the soil thermal regime, a large proportion of variance in soil temperature trends over the course of the experiment could be explained by pre-treatment temperatures across all experimental locations, which in turn appeared strongly related to timing of snowmelt (Fig. S14). Thickness of soil organic layers generally explained the second-largest proportion of environmental variability in soil temperature trends. Particularly in the wetter polygonal tundra site in Adventdalen, natural moisture variability appeared to mask the effect of the rainfall treatments (Fig. 5c) on ALT. Hence, we find that the influence of experimentally induced heavy rainfall events on the soil thermal regime is generally negligible compared to other sources of environmental variability, and the few observed effects were temporary and

site-specific.

4.1. Regional differences in rainfall sensitivity of permafrost

Our findings provide a stark contrast to earlier findings in continental Siberia (Lopez et al., 2010; Magnússon et al., 2022) and Alaska (Neumann et al., 2019; Douglas et al., 2020), where heavy rainfall events or artificial watering were observed to lead to substantial increases in permafrost thaw or soil temperatures. Similarly, ecosystem modeling evidence concludes that heat advection from infiltrating rainwater may generate as much warming of permafrost soils as air temperature warming for the Alaskan north Slope region (Mekonnen et al., 2021). However, several studies conducted in permafrost sites on the Tibet-Qinghai Plateau report a cooling effect of rainfall events on ground temperatures, attributed to increased latent heat loss, delayed response to air temperatures and reduced heat transport into the soil (Zhang et al., 2021; Zhou et al., 2021; Yang et al., 2023). Recent evidence from data synthesis and permafrost thermal-hydrological modeling (Hamm et al., 2023) suggests that permafrost situated in maritime climate zones may be less prone to accelerated thaw under heavy rainfall than continental permafrost, which is in line with our results. Model outcomes attribute the low sensitivity of maritime permafrost to additional rainfall to lower heat conduction under cooler, cloudier and wetter summer conditions and relatively high baseline soil moisture (Hamm et al., 2023). The latter aligns with the site-specific responses we observed in our study, where rainfall impacts (i.e. accelerated thaw in the Adventdalen loess terrace site and a tendency of topsoil cooling in the site in Ny-Ålesund, Fig. 4, S12a) were limited to drier soils (Fig. S5a) with a higher degree of effectuated wetting (Fig. S4). The above suggests that permafrost in other regions with relatively cool summers and wetter baseline conditions (such as parts of Greenland and the Tibetan plateau) (Hamm et al., 2023), may show similar insensitivity to rainfall extremes. Studies quantifying permafrost thaw progression under experimental irrigation in additional maritime permafrost sites or mountain permafrost regions at lower latitudes would be a valuable addition to the current knowledge base.

4.2. Role of seasonal timing and magnitude of rainfall events

Timing of heavy rainfall events relative to ambient air temperatures and seasonal thaw progression may co-determine the impact of rainfall on permafrost thaw. In a comparable irrigation study in Siberia (Magnússon et al., 2022), irrigation was supplied shortly after thaw onset with initial thaw depths (approximately 10 cm to 15 cm) shallower than in the present study (Fig. 2a). The relatively large effect of the first 30 mm of irrigation in early summer (Fig. 3) compared to absence of effects of late summer irrigation in 2022 (Table S21) would suggest a stronger rainfall response in the early thaw season. This could potentially be explained by larger heat conduction under wetting in soils with large gradients between soil and air temperature, or by rapid advection of heat from relatively warm rainfall or irrigation water to the shallow thaw front (Hamm et al., 2023). Similarly, earlier modeling results suggest no effect of late summer rainfall on active layer development, but stronger lagged effects in subsequent seasons (Magnússon et al., 2022). This is consistent with our observation of slower freeze-up and colder winter temperatures following irrigation in late summer 2022 (Figs. S7-S8, Tables S12-S15). However, comparing the effects of later and earlier summer rainfall application in 2023, thaw rates do not indicate a clear reduction in the effect of irrigation treatment over the summer season (Fig. 3, Table S23), suggesting that seasonal timing does not determine the magnitude of rainfall impacts on permafrost in a linear fashion. Alternatively, the timing of heavy rainfall events relative to concurrent ambient air temperature fluctuations may determine the effect size. Finally, higher thaw rates may be observed later in the summer season for sites with previously shallower thaw (Fig. 5a, S11c, d), suggesting that local early season acceleration of thaw may result in slower thaw progression later in the season. Detailed on-site monitoring of thaw progression, air temperatures, precipitation and heat fluxes combined with extensively parameterized physical modeling of soil thermal hydrology should help to disentangle the role of timing of rainfall events (Magnússon et al., 2022; Smith et al., 2022).

The intensity of rainfall may co-determine the relative amounts of added water subject to retention in the topsoil, evaporation and percolation (Table S4), each with contrasting implications for soil temperatures and permafrost thaw. Diverging responses of permafrost soil temperature and thaw depth have been observed among moderate and heavy rainfall events (Luo et al., 2020). Similarly, ALT and ground temperatures show mutually different and non-linear associations with annual rainfall amounts in a panarctic context (Karjalainen et al., 2019). This suggests that the influence of rainfall on permafrost thaw likely shows threshold dynamics or other non-linearities, and that responses of the shallow soil thermal regime may not be representative for temperature changes in the subsoil or dynamics of ALT (Karjalainen et al., 2019; Clayton et al., 2021; Hamm et al., 2023). Hence, care must be taken in extrapolating observed impacts of heavy rainfall events (as mimicked in this study) to scenarios of modest increases in rainfall and vice versa.

4.3. Local drivers of permafrost rainfall sensitivity

4.3.1. Role of vertical heat fluxes

Using field-measured irrigation water temperatures, surface to topsoil temperature gradients and moisture values, a simplified lysimeter set-up and commonly used soil thermal parameters (Text S1, Tables S2-S7), we approximated several vertical heat flux components under the irrigation treatments. While these do not represent actual field-measured heat fluxes, these estimates provide insight into the expected role of several vertical heat exchange processes under heavy rainfall events. In general we find comparatively small increases in heat advection (infiltration of relatively warm irrigation water) and conduction (due to topsoil wetting) as a result of irrigation, but comparatively large latent heat losses due to increased evaporation. Earlier work also found limited influence of water infiltration on permafrost thaw in Adventdalen (Schuh et al., 2017). Mismatches in thermal input due to the use of comparatively warm surface water during irrigation were found to be comparably minor (Table S2). Using a simplified lysimeter setup (Text S1.3), we estimated that around 40 % (observed range: 16–69 %) of water added through irrigation evaporated within the course of 4 days, which would effectuate a substantial cooling of the soil due to evaporative heat loss (Table S5). We find that evaporation rates in irrigated soil were several times higher than under ambient conditions. While our methods to estimate evaporation and heat fluxes were simple and indirect, polar desert environments may be expected to experience high evaporation due to high wind speed and low vegetation stature, and our observed evaporation rates and heat fluxes are approximately in line with values from Westermann et al. (2009). Of the added irrigation water, 0–59 % percolated to deeper soil layers within an hour (Table S4). We observed a higher degree of immediate percolation of rainwater under larger amounts of added irrigation water, and higher percolation rates in the mineral soils at the loess terrace site (Location 1) compared to lower rates in the predominantly organic soils at the polygonal tundra site (Location 2). The high rainfall intensity simulated in our experiment (10 mm was added in under half an hour) suggests that such rapid percolation may not be entirely representative, but does suggest that higher rainfall intensity, relatively warm rainfall temperatures and sandy soils with little organic materials are associated with higher advective warming due to deeper percolation of rainwater. This may help explain the observed acceleration of thaw rates for the loess terrace site. The small and short-duration effects observed for this site may be even smaller in reality due to colder temperature of ambient rainwater. In addition, natural rainfall events are associated with lower net radiation, which has been found to contribute to soil cooling (Zhang et al.,

2021). Changes to net radiation were not represented in our experimental set-up. Hence, our findings suggest a relatively minor role of direct and indirect thermal inputs with irrigation water, particularly in organic soils, and a relatively large role of evaporative cooling. This additionally suggests that moisture retention by topsoil and moss layers is an important driver of vertical heat exchange (Blok et al., 2011). This high evaporative heat loss compared to ground heat flux could help explain the relative lack of effect observed in this study. Similar dynamics may also explain the lower sensitivity of permafrost in maritime regions and the Qinghai-Tibet Plateau to heavy rainfall (Zhang et al., 2021; Hamm et al., 2023).

4.3.2. Role of local abiotic contrasts

The relatively small and localized impacts of simulated heavy rainfall events are likely also a result of our site selection. We chose sites to represent gradients in soil type and topography. While representative of the broader landscape, this did introduce variable amounts of within-site environmental heterogeneity that may have locally masked treatments effects. Only the relatively dry and hydrologically homogeneous location in Ny-Ålesund (Location 5, Figs. S4-S5) showed indications of diverging soil temperature trends under early summer irrigation (Fig. S8). In this site, evaporative cooling of the relatively dark and sparsely vegetated surfaces with mainly cryptogamic crusts (*Magnússon, Verhoeven, pers. obs.*) may explain the stronger cooling trend observed in shallow soil layers upon early summer irrigation (Fig. S13a). The sites in Endalen (Locations 3 & 4), which feature larger topographical contrasts, show high seasonal variation in soil moisture and temporary local inundation throughout the melt season (Figs. S4-S5) and no indication of variability in soil temperature trends among treatments (Fig. S12). Although lack of deeper soil temperatures and thaw depth data for these sites prevent conclusions regarding permafrost thaw in Endalen, the high natural variability in topography, snowmelt and water levels in these sites (Fig. S5) appears to overshadow any effectuated wetting through irrigation (Fig. S4). The irrigation treatment temporarily enhanced thaw rates at the relatively dry and homogeneous loess terrace site, but not in a wetter polygonal tundra area with higher within-site variability in soil moisture (Fig. 4, S4). Additionally, we observed standing water in polygon troughs (*pers. obs.*) and stronger association of active layer thickness with seasonally averaged soil moisture for the polygonal tundra site (Location 2, Fig. 5c). This suggests that natural moisture dynamics may mask the impact of treatment in more hydrologically dynamic landscape positions, or that the influence of topsoil moisture is limited compared to that of water table height.

Although we could not establish the date of snowmelt for all plots, local gradients in snowmelt timing likely induced additional variability in soil temperature trends and seasonal moisture dynamics. We found a relatively strong association of soil warming trends under treatment with pretreatment temperatures and topsoil moisture content in the early summer season (Fig. 5). In turn, for a selection of C & I plots for which snowmelt timing was recorded, we found strong association of pretreatment soil temperatures, soil moisture and temperature trends with timing of snowmelt in early summer (Fig. S14). Hence, these associations likely reflect a similar dynamic of colder and wetter conditions and faster warming in recently snow-free sites. Soil temperature curves confirm strong divergence in timing of thaw (up to a month) among and within study locations (Fig. 2). This role of thawing season onset, snow depth and cover duration is well documented in permafrost monitoring sites across the Scandinavian Arctic and Greenland (Christiansen, 2004; Åkerman and Johansson, 2008; Strand et al., 2021). In line with our findings, different degrees of variability in snow cover duration and climatic conditions among monitoring sites have been found to lead to regional and local differences in the relative importance of climatic drivers of permafrost thaw (Strand et al., 2021).

4.3.3. Role of local biotic contrasts

Additionally, vegetation and organic soil properties may contribute to regional and local contrasts in rainfall response of permafrost. Contrary to earlier studies (Blok et al., 2011; Gornall et al., 2007), we found little indication of biotic controls on thaw, nor regulation of rainfall response by such biotic factors (Fig. 5). Deeper organic layers did appear to be associated with slower soil warming, particularly in the earlier thaw season (Fig. 5b, S12), but did not show interaction with rainfall response (Fig. 5). This cooling role of organic layers is well established in earlier permafrost studies (Jorgenson et al., 2010; Johnson et al., 2013; Atchley et al., 2015). Gornall et al. (2007) report a substantial cooling effect and delay of thaw under increasing moss height in Adventdalen, Svalbard, but similar end-of-season active layer thickness. Moss heights observed in our sites (generally below 3 cm, Figs. S11-S12) were low compared to those reported in Gornall et al. (2007). Similarly, we observe very limited overall values and variability in vegetation height (generally below 6 cm, Figs. S11-S12). This may have contributed to the low association of vegetation properties with soil thermal regime or rainfall response (Fig. 5) compared to an earlier study on Svalbard (Gornall et al., 2007). The influence of vegetation canopies may differ in Low Arctic settings, where taller vegetation structures may exert more control on ground shading in summer and snow trapping in winter (Domine et al., 2016; Grunberg et al., 2020; Heijmans et al., 2022) and additionally modulate permafrost rainfall response through interception of rainfall (Zwieback et al., 2019). Hence, the low association of vegetation with the soil thermal regime and its apparently negligible role in rainfall sensitivity of permafrost observed in this study should likely also be viewed in the context of the generally limited stature of High Arctic vegetation.

4.4. Implications of increased heavy rainfall across heterogeneous permafrost environments

Substantial evaporative heat loss (*see 4.3.1*, Fig. S2) and a low degree of effectuated wetting (Fig. S4) were discussed as potential mechanisms underlying the comparative insensitivity of the soil thermal regime to experimental rainfall on Svalbard. Additional sources of heterogeneity permafrost environments, such as soil texture, moisture retention (Smith et al., 2022) and ground ice content, likely affect their susceptibility to rainfall extremes. Permafrost degradation in ice-rich permafrost may lead to a positive feedback due to snow and water accumulation in locally subsided areas with deeper position of the permafrost table (Nauta et al., 2015). Ice content of Svalbard permafrost is generally lower (Brown et al., 1997), although excess ground ice is present locally in our study region (e.g. in our polygonal tundra study site) (Christiansen et al., 2021). This implies that the role of thermokarst is generally less pronounced on Svalbard, but potentially relevant in permafrost-rainfall response in other Arctic regions. In combination with a deeper permafrost table on Svalbard, this could help explain why similar irrigation treatments in an ice-rich Siberian tundra site led to build-up of internal water tables on top of a shallow and locally heterogeneous thaw front, and substantial carry-over effects in following years (Magnússon et al., 2022), while no carry-over effects were observed in the present study. Carry-over effects from the 2023 irrigation sessions or from the 2022 treatments in later years cannot be formally ruled out, although the comparative absence of same- and next-season effects provides little mechanistic basis for their later occurrence. These contrasting findings suggest that the degree of feedback and duration of rainfall effects likely varies regionally or locally, which may also require variable duration of monitoring after experimental interventions or extreme events.

Earlier watering experiments in the Siberian Arctic that found significant and pronounced acceleration of thaw upon wetting featured study set-ups with a single location or environmentally homogeneous conditions (Lopez et al., 2010; Magnússon et al., 2022), in contrast to our deliberate inclusion of local landscape variability. In the present study, effects of experimental rainfall increases appeared to be more evident in experimental sites with homogeneous conditions. This

suggests that the inclusion of environmental gradients is a key consideration in experimental design of future monitoring and manipulation studies of climate impacts on permafrost. A multi-year monitoring study of active layer thickness across pronounced environmental gradients in Fairbanks, Alaska, did find a spatially consistent and significant increase in thaw depth in rainier summers, but also featured a high degree of within-site replication (Douglas et al., 2020). While single area, homogeneous study set-ups may disregard landscape variability in climatic sensitivity of permafrost, studies that do include environmental gradients require detailed understanding of local sources of environmental heterogeneity to select appropriate subsites and replication levels.

Lastly, apart from local effects evident from manipulation studies such as ours, landscape-scale hydrology and lateral flow could substantially govern the impacts of natural heavy rainfall events. Particularly in a topographically diverse environment such as Svalbard, lateral flow and redistribution of water under natural heavy rainfall events could result in redistribution of thermal effects throughout the landscape (Hamm and Frampton, 2021). This would likely affect seasonal associations between soil moisture, soil thermal dynamics and permafrost thaw depth, and could manifest as locally augmented effects in natural concentration points for water flow through the active layer (Wright et al., 2009; Neumann et al., 2019; Eklof et al., 2024). The effects of top-down wetting from rainfall on permafrost thaw may additionally differ from the effects of local water tables dynamics and lateral flow due to contrasting roles of latent heat requirements, evaporative cooling, topsoil heat conduction and heat advection (Clayton et al., 2021; Hamm and Frampton, 2021). In the present study only topsoil moisture was monitored and lateral flow could not be quantified. Lateral flow was likely minimal in the Loess terrace site (Schuh et al., 2017), and likely confined by ice-wedge structures in the polygonal tundra site. Lateral redistribution of irrigation water in the slope sites (particularly in Location 4, Endalen) cannot be ruled out, but based on field observations of seasonal soil moisture dynamics (Fig. S4), such effects were likely overshadowed by natural variability in lateral flow, particularly during periods of high snowmelt. More detailed monitoring of subsurface soil moisture profiles and use of frost tubes to monitor thaw depths in rocky terrain would help assess the importance of subsurface flow and associated thermal-hydrological processes. Finally, the combined effects of heavy rainfall and deepening of the active layer may result in solifluction and landslides (Hanssen-Bauer et al., 2019; Christiansen et al., 2021). Although in the present set-up the impact of extreme rainfall was limited, locally augmented impacts through topographical redistribution of water and heat and erosion may be expected under natural rainfall extremes.

5. Conclusion & recommendations

Although a local and short-lived acceleration of thaw was observed under experimental rainfall increase, our work fits emerging evidence that permafrost situated in high-Arctic sites with maritime climates (e.g. Svalbard, coastal Greenland) are less sensitive to degradation under heavy rainfall events than permafrost situated in continental, lower Arctic settings (e.g. inland Alaska and Siberia). This implies that future increases in heavy rainfall events in summer on Svalbard are unlikely to cause ubiquitous and persistent increases in permafrost thaw, and that other climate and landscape factors exert a stronger influence on permafrost thermal regimes in this region. Timing of thaw onset (related to snowmelt timing) in particular showed strong association with observed thaw rates and soil temperature trends. To properly constrain permafrost rainfall sensitivity across regions and landscapes, replicated experimental irrigation set-ups that allow for better control of irrigation rates and water temperatures (Grysko et al., 2021; Renner et al., 2024) across Arctic regions (including High and Low Arctic sites) and natural landscape gradients would be necessary, although this is logistically challenging. A drawback of such an approach is that smaller-scale experimental irrigation disregards the role of natural redistribution of rainfall within the landscape through lateral flow within the active layer. Monitoring of thaw progression, soil moisture and soil temperature across hydrological gradients under natural rainfall extremes, ideally supported by 2D or 3D model simulation of permafrost hydrology, would help disentangle how various thermal-hydrological mechanisms shape the impact of heavy rainfall events on permafrost in various settings, and how rainfall and its thermal effects are distributed hydrologically throughout permafrost landscapes. Lastly, improved availability of long-term on-site rainfall and soil moisture profiles at existing permafrost monitoring facilities would help to develop a pan-arctic perspective on the rainfall sensitivity of permafrost.

Funding

Fieldwork was funded through Arctic Field Grants of the Research Council of Norway (Svalbard Science Forum, grant numbers 342019, 342049, 342016 & 342153) and the KNAW Ecology Fund Grant of the Royal Netherlands Academy of Arts & Sciences (Grant number KNAWWF/255/2023021). The research leading to these results has received funding from the European Union's Horizon 2020 project INTERACT, under grant agreement No 871120. Mo Verhoeven is part of the Vulnerability of Arctic migratory birds to rapid climate change research consortium funded by the Netherlands Polar Programme (NPP) of the Dutch Research Council (NWO). Additional financial support from the Plant Ecology & Nature Conservation Group (WUR) and logistic and material support from UNIS Arctic Biology, the Netherlands Arctic Station and AWIPEV are gratefully acknowledged.

CRediT authorship contribution statement

R.Í. Magnússon: Conceptualization, Data curation, Formal analysis, Funding acquisition, Investigation, Methodology, Project administration, Visualization, Writing – original draft, Writing – review & editing. **S. Schuuring:** Conceptualization, Investigation, Resources, Writing – review & editing. **A. Hamm:** Conceptualization, Investigation, Resources, Writing – review & editing. **M.A. Verhoeven:** Conceptualization, Investigation, Resources, Writing – review & editing. **J. Limpens:** Conceptualization, Investigation, Methodology, Writing – review & editing. **M.J.E.E. Loonen:** Conceptualization, Resources, Writing – review & editing. **S.I. Lang:** Conceptualization, Funding acquisition, Investigation, Methodology, Project administration, Resources, Supervision, Writing – review & editing.

Declaration of competing interest

The authors declare that they have no known competing financial interests or personal relationships that could have appeared to influence the work reported in this paper.

Data availability

Datasets and code used for this study are available from the DANS EASY repository (https://doi.org/10.17026/dans-23v-7hcg). Datasets, project updates and fieldwork permits are available on the Research in Svalbard database (www.researchinsvalbard.no) under project numbers 11968 and 12016.

Acknowledgements

Field activities were supported by Christian Menheere, Michiel Bontje, Manon van den Dolder, Violet van Rooijen, Carla Suñol-Escribano (WUR, UNIS), Anne Vorenkamp, Pyter Bootsma, Roos Winters, Lisa Schleijpen, Susanne Hoogsteen, Maaike Everts (RUG, Arctic Centre), Eric Schytt Mannerfelt and Anna Johansson (Stockholm University).

Appendix A. Supplementary data

Supplementary data to this article can be found online at https://doi.org/10.1016/j.scitotenv.2024.173696.

References

Åkerman, H.J., Johansson, M., 2008. Thawing permafrost and thicker active layers in sub-arctic Sweden. Permafr. Periglac. Process. 19, 279–292.

AMAP, 2021. Arctic Climate Change Update 2021: Key Trends and Impacts. Summary for Policy-makers, Tromsø, Norway.

Atchley, A.L., Painter, S.L., Harp, D.R., Coon, E.T., Wilson, C.J., Liljedahl, A.K., Romanovsky, V.E., 2015. Using field observations to inform thermal hydrology models of permafrost dynamics with ATS (v0. 83). Geosci. Model Dev. 8, 2701–2722.

Bates, D., Mächler, M., Bolker, B., Walker, S., 2015. Fitting linear mixed-effects models using lme4. J. Stat. Softw. 67, 1–48.

Bintanja, R., Andry, O., 2017. Towards a rain-dominated Arctic. Nat. Clim. Chang. 7, 263–267.

Bintanja, R., van der Wiel, K., Van der Linden, E., Reusen, J., Bogerd, L., Krikken, F., Selten, F., 2020. Strong future increases in Arctic precipitation variability linked to poleward moisture transport. Sci. Adv. 6, eaax6869.

Biskaborn, B.K., Smith, S.L., Noetzli, J., Matthes, H., Vieira, G., Streletskiy, D.A., Schoeneich, P., Romanovsky, V.E., Lewkowicz, A.G., Abramov, A., 2019. Permafrost is warming at a global scale. Nat. Commun. 10, 1–11.

Blok, D., Heijmans, M., Schaepman-Strub, G., van Ruijven, J., Parmentier, F., Maximov, T., Berendse, F., 2011. The cooling capacity of mosses: controls on water and energy fluxes in a Siberian tundra site. Ecosystems 14, 1055–1065.

Boike, J., Juszak, I., Lange, S., Chadburn, S., Burke, E., Overduin, P.P., Roth, K., Ippisch, O., Bornemann, N., Stern, L., 2018. A 20-year record (1998–2017) of permafrost, active layer and meteorological conditions at a high Arctic permafrost research site (Bayelva, Spitsbergen). Earth Syst. Sci. Data 10, 355–390.

Brown, J., Ferrians Jr., O., Heginbottom, J.A., Melnikov, E., 1997. Circum-arctic Map of Permafrost and Ground-ice Conditions. US Geological Survey Reston, VA.

Christensen, T., Lund, M., Skov, K., Abermann, J., Lopez-Blanco, E., Scheller, J., Scheel, M., Jackowicz-Korczynski, M., Langley, K., Murphy, M., 2021. Multiple ecosystem effects of extreme weather events in the Arctic. Ecosystems 24, 122–136.

Christiansen, H.H., 2004. Meteorological control on interannual spatial and temporal variations in snow cover and ground thawing in two northeast Greenlandic Circumpolar-Active-Layer-Monitoring (CALM) sites. Permafr. Periglac. Process. 15, 155–169.

Christiansen, H.H., Gilbert, G.L., Neumann, U., Demidov, N., Guglielmin, M., Isaksen, K., Osuch, M., Boike, J., 2021. Ground ice content, drilling methods and equipment and permafrost dynamics in Svalbard 2016–2019 (PermaSval). In: SESS Report 2020-The State of Environmental Science in Svalbard-An Annual Report, p. 3.

Clayton, L.K., Kevin, S., Michael, J.B., Laura, B.-C., Jingyi, C., Richard, H.C., Albert, C.C., Kazem, B.-D., Sarah, G., Elchin, J., Lin, L., Roger John, M., Mahta, M., Andrew, P., Adrian, V.R., Sean, R.S., Taylor, S., Alireza, T., Kang, W., Cathy, J.W., Howard, A.Z., Tingjun, Z., Yuhuan, Z., 2021. Active layer thickness as a function of soil water content. Environ. Res. Lett. 16, 055028.

Domine, F., Barrere, M., Morin, S., 2016. The growth of shrubs on high Arctic tundra at Bylot Island: impact on snow physical properties and permafrost thermal regime. Biogeosciences 13, 6471–6486.

Douglas, T.A., Turetsky, M.R., Koven, C.D., 2020. Increased rainfall stimulates permafrost thaw across a variety of interior Alaskan boreal ecosystems. npj Clim. Atmos. Sci. 3, 1–7.

Eklof, J., Jones, B.M., Dafflon, B., Devoie, E., Ring, K., English, M., Waldrop, M., Neumann, R.B., 2024. Canopy cover and microtopography control precipitation-enhanced thaw of ecosystem-protected permafrost. Environ. Res. Lett. 19, 044055.

Gornall, J.L., Jonsdottir, I.S., Woodin, S.J., Van der, R., et al., 2007. Arctic mosses govern below-ground environment and ecosystem processes. Oecologia 153, 931–941.

Grömping, U., 2007. Relative importance for linear regression in R: the package relaimpo. J. Stat. Softw. 17, 1–27.

Grunberg, I., Wilcox, E.J., Zwieback, S., Marsh, P., Boike, J., 2020. Linking tundra vegetation, snow, soil temperature, and permafrost. Biogeosciences 17, 4261–4279.

Grysko, R., Plekhanova, E., Oehri, J., Karsanaev, S.V., Maximov, T.C., Schaepman-Strub, G., 2021. Design of the tundra rainfall experiment (TRainEx) to simulate future summer precipitation scenarios. MethodsX 8, 101331.

Halekoh, U., Højsgaard, S., 2014. A kenward-roger approximation and parametric bootstrap methods for tests in linear mixed models–the R package pbkrtest. J. Stat. Softw. 59, 1–30.

Hamm, A., Frampton, A., 2021. Impact of lateral groundwater flow on hydrothermal conditions of the active layer in a high-Arctic hillslope setting. Cryosphere 15, 4853–4871.

Hamm, A., Magnússon, R.Í., Khattak, A.J., Frampton, A., 2023. Continentality determines warming or cooling impact of heavy rainfall events on permafrost. Nat. Commun. 14, 3578.

Hanssen-Bauer, I., Førland, E., Hisdal, H., Mayer, S., Sandø, A.B., Sorteberg, A., 2019. Climate in Svalbard 2100. A Knowledge Base for Climate Adaptation, p. 470.

Heijmans, M.M., Magnússon, R.Í., Lara, M.J., Frost, G.V., Myers-Smith, I.H., van Huissteden, J., Jorgenson, M.T., Fedorov, A.N., Epstein, H.E., Lawrence, D.M., 2022. Tundra vegetation change and impacts on permafrost. Nat. Rev. Earth Environ. 3, 68–84.

Hjort, J., Streletskiy, D., Doré, G., Wu, Q., Bjella, K., Luoto, M., 2022. Impacts of permafrost degradation on infrastructure. Nat. Rev. Earth Environ. 3, 24–38.

Hugelius, G., Strauss, J., Zubrzycki, S., Harden, J.W., Schuur, E.A.G., Ping, C.L., Schirrmeister, L., Grosse, G., Michaelson, G.J., Koven, C.D., O'Donnell, J.A., Elberling, B., Mishra, U., Camill, P., Yu, Z., Palmtag, J., Kuhry, P., 2014. Estimated stocks of circumpolar permafrost carbon with quantified uncertainty ranges and identified data gaps. Biogeosciences 11, 6573–6593.

Humlum, O., Instanes, A., Sollid, J.L., 2003. Permafrost in Svalbard: a review of research history, climatic background and engineering challenges. Polar Res. 22, 191–215.

Hyndman, R.J., Khandakar, Y., 2008. Automatic time series forecasting: the forecast package for R. J. Stat. Softw. 27, 1–22.

Iijima, Y., Fedorov, A.N., Park, H., Suzuki, K., Yabuki, H., Maximov, T.C., Ohata, T., 2010. Abrupt increases in soil temperatures following increased precipitation in a permafrost region, central Lena River basin, Russia. Permafr. Periglac. Process. 21, 30–41.

IPCC, 2021. Climate Change 2021: The Physical Science Basis. Contribution of Working Group I to the Sixth Assessment Report of the Intergovernmental Panel on Climate Change. Cambridge University Press, Cambridge, United Kingdom and New York, NY, USA.

Isaksen, K., Lutz, J., Sørensen, A.M., Godøy, Ø., Ferrighi, L., Eastwood, S., Aaboe, S., 2022. Advances in operational permafrost monitoring on Svalbard and in Norway. Environ. Res. Lett. 17, 095012.

Johnson, K.D., Harden, J.W., McGuire, A.D., Clark, M., Yuan, F., Finley, A.O., 2013. Permafrost and organic layer interactions over a climate gradient in a discontinuous permafrost zone. Environ. Res. Lett. 8, 035028.

Jorgenson, M., Romanovsky, V., Harden, J., Shur, Y., O'Donnell, J., Schuur, E.A., Kanevskiy, M., Marchenko, S., 2010. Resilience and vulnerability of permafrost to climate change. Can. J. For. Res. 40, 1219–1236.

Karjalainen, O., Luoto, M., Aalto, J., Hjort, J., 2019. New insights into the environmental factors controlling the ground thermal regime across the Northern Hemisphere: a comparison between permafrost and non-permafrost areas. Cryosphere 13, 693–707.

Kokelj, S., Tunnicliffe, J., Lacelle, D., Lantz, T., Chin, K., Fraser, R., 2015. Increased precipitation drives mega slump development and destabilization of ice-rich permafrost terrain, northwestern Canada. Global Planet. Change 129, 56–68.

Kusunoki, S., Mizuta, R., Hosaka, M., 2015. Future changes in precipitation intensity over the Arctic projected by a global atmospheric model with a 60-km grid size. Polar Sci. 9, 277–292.

Kuznetsova, A., Brockhoff, P.B., Christensen, R.H.B., 2017. lmerTest package: tests in linear mixed effects models. J. Stat. Softw. 82.

Lenth, R., 2024. emmeans: Estimated Marginal Means, aka Least-Squares Means. R package.

Lindeman, R.H., Merenda, P.F., Gold, R.Z., 1980. Introduction to Bivariate and Multivariate Analysis. Scott, Foresman Glenview, IL.

Lopez, C., Shirota, T., Iwahana, G., Koide, T., Maximov, T., Fukuda, M., Saito, H., 2010. Effect of increased rainfall on water dynamics of larch (Larix cajanderi) forest in permafrost regions, Russia: an irrigation experiment. J. For. Res. 15, 365–373.

Luo, D., Jin, H., Bense, V.F., Jin, X., Li, X., 2020. Hydrothermal processes of near-surface warm permafrost in response to strong precipitation events in the headwater area of the Yellow River, Tibetan Plateau. Geoderma 376, 114531.

Magnússon, R.Í., Hamm, A., Karsanaev, S.V., Limpens, J., Kleijn, D., Frampton, A., Maximov, T.C., Heijmans, M.M., 2022. Extremely wet summer events enhance permafrost thaw for multiple years in Siberian tundra. Nat. Commun. 13, 1–10.

Mekonnen, Z.A., Riley, W.J., Grant, R.F., Romanovsky, V.E., 2021. Changes in precipitation and air temperature contribute comparably to permafrost degradation in a warmer climate. Environ. Res. Lett. 16, 024008.

Miccadei, E., Piacentini, T., Berti, C., 2016. Geomorphological features of the Kongsfjorden area: Ny-Ålesund, Blomstrandøya (NW Svalbard, Norway). Rendiconti Lincei 27, 217–228.

Miner, K.R., Turetsky, M.R., Malina, E., Bartsch, A., Tamminen, J., McGuire, A.D., Fix, A., Sweeney, C., Elder, C.D., Miller, C.E., 2022. Permafrost carbon emissions in a changing Arctic. Nat. Rev. Earth Environ. 3, 55–67.

Nakagawa, S., Schielzeth, H., 2013. A general and simple method for obtaining R2 from generalized linear mixed-effects models. Methods Ecol. Evol. 4, 133–142.

Natali, S.M., Holdren, J.P., Rogers, B.M., Treharne, R., Duffy, P.B., Pomerance, R., MacDonald, E., 2021. Permafrost carbon feedbacks threaten global climate goals. Proc. Natl. Acad. Sci. 118, e2100163118.

Nauta, A.L., Heijmans, M.M., Blok, D., Limpens, J., Elberling, B., Gallagher, A., Li, B., Petrov, R.E., Maximov, T.C., Van Huissteden, J., 2015. Permafrost collapse after shrub removal shifts tundra ecosystem to a methane source. Nat. Clim. Chang. 5, 67.

Neumann, R.B., Moorberg, C.J., Lundquist, J.D., Turner, J.C., Waldrop, M.P., McFarland, J.W., Euskirchen, E.S., Edgar, C.W., Turetsky, M.R., 2019. Warming effects of spring rainfall increase methane emissions from thawing permafrost. Geophys. Res. Lett. 46, 1393–1401.

Obu, J., 2021. How much of the Earth's surface is underlain by permafrost? J. Geophys. Res. Earth 126, e2021JF006123.

Outcalt, S.I., Nelson, F.E., Hinkel, K.M., 1990. The zero-curtain effect: heat and mass transfer across an isothermal region in freezing soil. Water Resour. Res. 26, 1509–1516.

Renner, C., Conroy, N., Thaler, E., Collins, A., Thomas, L., Dillard, S., Rowland, J., Bennett, K., 2024. The next-generation ecosystem experiment Arctic rainfall simulator: a tool to understand the effects of changing rainfall patterns in the Arctic. Hydrol. Res. 55, 67–82.

Schuh, C., Frampton, A., Christiansen, H.H., 2017. Soil moisture redistribution and its effect on inter-annual active layer temperature and thickness variations in a dry loess terrace in Adventdalen, Svalbard. Cryosphere 11, 635–651.

Schuur, E.A., Abbott, B.W., Commane, R., Ernakovich, J., Euskirchen, E., Hugelius, G., Grosse, G., Jones, M., Koven, C., Leshyk, V., 2022. Permafrost and climate change: carbon cycle feedbacks from the warming Arctic. Annu. Rev. Env. Resour. 47, 343–371.

Smith, S.L., O'Neill, H.B., Isaksen, K., Noetzli, J., Romanovsky, V.E., 2022. The changing thermal state of permafrost. Nat. Rev. Earth Environ. 3, 10–23.

Stoffel, M.A., Nakagawa, S., Schielzeth, H., 2021. partR2: partitioning R2 in generalized linear mixed models. PeerJ 9, e11414.

Strand, S.M., Christiansen, H.H., Johansson, M., Åkerman, J., Humlum, O., 2021. Active layer thickening and controls on interannual variability in the Nordic Arctic compared to the circum-Arctic. Permafr. Periglac. Process. 32, 47–58.

Streletskiy, D., Noetzli, J., Smith, S.L., Vieira, G., Schoeneich, P., Hrbacek, F., Irrgang, A. M., 2022. Measurement Recommendations and Guidelines for the Global Terrestrial Network for Permafrost (GTN-P).

Tarnocai, C., Canadell, J., Schuur, E.A., Kuhry, P., Mazhitova, G., Zimov, S., 2009. Soil organic carbon pools in the northern circumpolar permafrost region. Global Biogeochem. Cycles 23, GB2023.

Teufel, B., Sushama, L., 2019. Abrupt changes across the Arctic permafrost region endanger northern development. Nat. Clim. Chang. 9, 858–862.

Von Oppen, J., Assmann, J.J., Bjorkman, A.D., Treier, U.A., Elberling, B., Nabe-Nielsen, J., Normand, S., 2022. Cross-scale regulation of seasonal microclimate by vegetation and snow in the Arctic tundra. Glob. Chang. Biol. 28, 7296–7312.

Westermann, S., Lüers, J., Langer, M., Piel, K., Boike, J., 2009. The annual surface energy budget of a high-arctic permafrost site on Svalbard, Norway. Cryosphere 3, 245–263.

Wright, N., Hayashi, M., Quinton, W.L., 2009. Spatial and temporal variations in active layer thawing and their implication on runoff generation in peat-covered permafrost terrain. Water Resour. Res. 45, W05414.

Yang, J., Wang, T., Yang, D., 2023. Divergent responses of permafrost degradation to precipitation increases at different seasons on the eastern Qinghai–Tibet Plateau based on modeling approach. Environ. Res. Lett. 18, 094038.

Zhang, M., Wen, Z., Li, D., Chou, Y., Zhou, Z., Zhou, F., Lei, B., 2021. Impact process and mechanism of summertime rainfall on thermal–moisture regime of active layer in permafrost regions of central Qinghai–Tibet Plateau. Sci. Total Environ. 796, 148970.

Zhou, Z.-x., Zhou, F.-x., Zhang, M.-l., Lei, B.-b., Ma, Z., 2021. Effect of increasing rainfall on the thermal—moisture dynamics of permafrost active layer in the central Qinghai—Tibet Plateau. J. Mt. Sci. 18, 2929–2945.

Zwieback, S., Chang, Q.Y., Marsh, P., Berg, A., 2019. Shrub tundra ecohydrology: rainfall interception is a major component of the water balance. Environ. Res. Lett. 14, 055005.